ACES Asian Chemical Editorial Society

DOI: 10.1002/asia.201600116

CHEMISTRY AN ASIAN JOURNAL Full Paper

Structure–Activity Relationships

# Solution and Solid-State Analysis of Binding of 13-Substituted Berberine Analogues to Human Telomeric G-quadruplexes

Marta Ferraroni,[a] Carla Bazzicalupi,*[a] Francesco Papi,[a, b] Gaetano Fiorillo,[c] Luis Miguel Guamán-Ortiz,[d, e] Alessio Nocentini,[b] Anna Ivana Scovassi,[e] Paolo Lombardi,[c] and Paola Gratteri*[b]

**Abstract:** The interaction between 13-phenylalkyl and 13-diphenylalkyl berberine derivatives (**NAX**) and human telomeric DNA G4 structures has been investigated by both spectroscopic and crystallographic methods. **NAX042** and **NAX053** are the best compounds improving the performance of the natural precursor berberine. This finding is in agreement with the X-ray diffraction result for the **NAX053**-Tel12 adduct, showing the ligand which interacts via π-stacking, sandwiched at the interface of two symmetry-related quadruplex units, with its benzhydryl group contributing to the overall stability of the adduct by means of additional π-stacking interactions with the DNA residues. The berberine derivatives were also investigated for their cytotoxic activity towards a panel of human cancer cell lines. Compounds **NAX042** and **NAX053** affect the viability of cancer cell lines in a dose-dependent manner.

## Introduction

G-quadruplex (G4) structures are higher-order nucleic acid arrangements formed by G-rich sequences present at the end of linear eukaryotic chromosomes and at various promoter regions of oncogenes (e.g., c-myc and c-kit).[1] G4 are four-stranded, intra- or inter- molecular architectures, characterized by planes of four guanine residues interacting through Hoogsteen hydrogen bonds which stack on each other by means of π–π stacking interactions, giving rise to a variety of foldings. Monovalent metal ions, such as $Na^+$ and $K^+$, are found in the channel formed by the guanine residues contributing to the resulting stability of the structure.[1f]

G4 has become a subject of great interest during the past decade because of its involvement in genome integrity and gene expression.[2] The folding of single-stranded telomeric DNA into a G4 structure inhibits telomerase, an enzyme highly overexpressed in cancer cells that effectively makes them immortal by preventing telomere shortening and, as a consequence, cell senescence.[3] Moreover, the biological relevance of G4, supported by the direct visualization of G4 DNAs and RNAs in human cells,[4] has attracted great interest. Many efforts were addressed to search ligand compounds able to induce and stabilize telomeric G4[5] and able to selectively target G-quadruplexes over dsDNA, in order to decrease the debilitating collateral effects which are normally associated with classical chemotherapies.[6]

Berberine (BER) (Scheme 1) is a natural isoquinoline quaternary alkaloid isolated from many plants of Chinese traditional medicines, such as *Coptis chinensis* and *Hydrastis canadensis*.[7] The compound shows multiple pharmacological effects,[7–9] including anticancer activity, possibly deriving from its ability to form complexes with nucleic acids, induce DNA damage, and exert related effects such as telomerase inhibition, topoisomerase poisoning, and inhibition of gene transcription. Recently, it has been demonstrated that BER binds and stabilizes human telomeric G4.[10–12]

BER matches the requirements to be a quadruplex binder, having an extended π-delocalized system along with a positive charge.[5] Several derivatives have been developed from its scaffold to enhance the overall DNA binding efficacy through appropriate functionalizations.[13] Substitutions in 9 and 13 positions were found to enhance the anticancer activity and the

[a] *Dr. M. Ferraroni, Prof. C. Bazzicalupi, Dr. F. Papi*
*Department of Chemistry*
*University of Florence*
*Via della Lastruccia 3, 50019 Sesto Fiorentino (FI) (Italy)*
*E-mail: carla.bazzicalupi@unifi.it*

[b] *Dr. F. Papi, Dr. A. Nocentini, Prof. P. Gratteri*
*Department NEUROFARBA—Pharmaceutical and nutraceutical section*
*Laboratory of Molecular Modeling Cheminformatics&QSAR*
*University of Firenze*
*via Ugo Schiff 6, 50019 Sesto Fiorentino, Firenze (Italy)*
*E-mail: paola.gratteri@unifi.it*

[c] *Dr. G. Fiorillo, Dr. P. Lombardi*
*Naxospharma srl*
*via G. Di Vittorio, 70, 20026 Novate Milanese (Italy)*

[d] *Dr. L. M. Guamán-Ortiz*
*Universidad Técnica Particular de Loja*
*Departamento de Ciencias de la Salud*
*San Cayetano Alto, Calle Paris, 1101608 Loja (Ecuador)*

[e] *Dr. L. M. Guamán-Ortiz, Dr. A. I. Scovassi*
*Istituto di Genetica Molecolare del CNR*
*Via Abbiategrasso 207, 27100, Pavia (Italy)*

*Supporting information and the ORCID identification number(s) for the author(s) of this article can be found under http://dx.doi.org/10.1002/asia.201600116.*

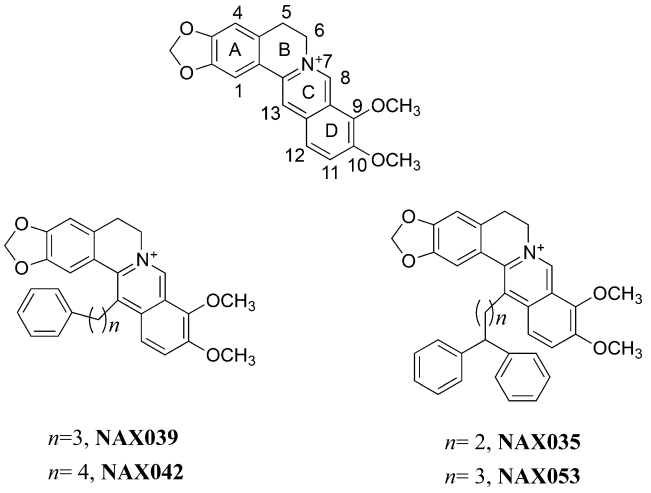


**Scheme 1.** Chemical structure of berberine (BER) and the 13-phenylalkyl and 13-diphenylalkyl berberine derivatives studied in this work.

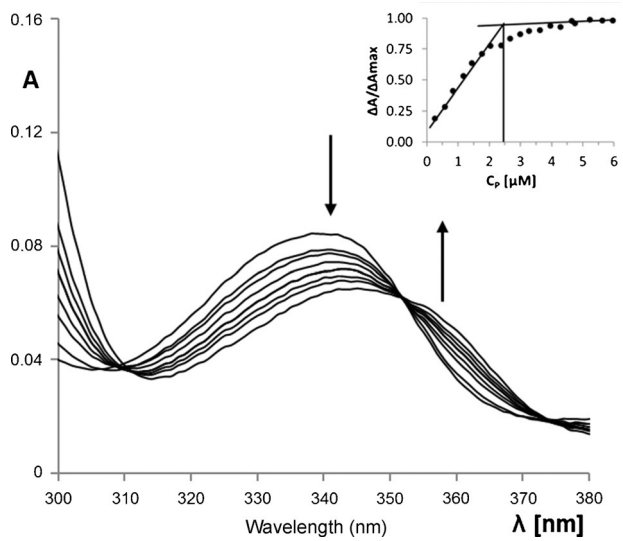


**Figure 1.** UV/Vis absorption spectra of 3.9 μM **NAX053** in the presence of increasing concentrations of Tel24 in 10 mM potassium phosphate buffer containing 150 mM KCl at pH 7 at 25 °C. Curves shown in the plot are relative to the addition of DNA between 0 and 0.6 equivalents with respect to the ligand. Inset: binding stoichiometry obtained from the intersection of the straight lines representing the linear fit of the initial and final data points of the binding isotherm.

G4 stabilizing activity as compared with BER.[14] The present work is aimed at investigating a set of berberine-related compounds bearing either a phenyl group or a benzhydryl group linked to position 13 of the berberine skeleton, through a hydrocarbon linker of variable length (Scheme 1).

This derivatization might generate a geometric propensity for additional stacking-type, non-covalent aromatic interactions with cellular targets. It is well known that aromatic interactions are ubiquitous in nature and that their geometry plays a central role in the molecular interaction with biological macromolecules.[15] Previous studies dealing with the elucidation of both dsDNA and RNA interaction modes of these structurally new derivatives (Scheme 1)[16–19] provided evidence of the contribution of the (di)phenylalkyl appendage to form stronger complexes with nucleic acids than BER.

Aiming at shedding light on the binding features of the BER derivatives on the human telomeric DNA G4 structures, we performed solution and solid-state characterization, using UV/Vis and CD spectroscopic methods and X-ray crystallography.

## Results and Discussion

### UV/Vis Absorption Spectroscopy

The presence of interactions between Tel24 d[$(T_2AG_3)_4$] and berberine analogues was investigated by absorption measurements. UV/Vis titrations were performed in order to obtain an estimation of both the binding strength, as dissociation constant $K_d$, and the ligand:quadruplex stoichiometry. Additionally, titrations for the reference compound BER were carried out by applying the same experimental conditions used for the studied compounds. Upon binding, the absorption peak evidenced hypochromic and bathochromic effects (Figure 1 and Figure S1), and the appearance of an isosbestic point in the range of 350–355 nm was observed, suggesting the presence of a single ligand–quadruplex adduct species over the entire concentration range investigated. The observed red-shift could be explained in terms of stabilization of the π* orbital of the ligands as a consequence of strong π–π interactions with the G-quartets of the receptor.[20,21] These data are in agreement with those reported in the literature for BER and other low-molecular-weight ligands interacting with G-quadruplex structures.[10b,20,21]

The variation in absorbance at about 340 nm for the ligands was analyzed as a function of increasing DNA concentration in order to estimate the dissociation constant $K_d$ and the ligand:quadruplex stoichiometric ratio of the resulting adducts, following previously described methods.[20–22] Further details are reported in the Experimental Section. Results of UV/Vis titrations are summarized in Table 1.

Titrations have been performed also for BER in order to obtain reference $K_d$ and stoichiometry ratio under the experimental conditions used ($K_d = 8.6 \cdot 10^{-6}$ M; binding stoichiometry

**Table 1.** Dissociation constants $K_d$ and stoichiometry ratio for the interaction of Tel24 with berberine and its 13-monophenyl and 13-diphenylalkyl derivatives in 10 mM potassium phosphate buffer (pH 7) containing 150 mM KCl. Data were obtained by UV/Vis absorbance spectroscopy at 25 °C (e.s.d. in parentheses).

| Ligand | Carbons in the alkyl chain | Phenyl pendant groups | $K_d$ [μM] | Ligand:Quadruplex binding stoichiometry |
|---|---|---|---|---|
| **BER**, berberine | – | – | 9(1) | 1:1 |
| **NAX039** | 3 | 1 | 3.2(5) | 2:1 |
| **NAX042** | 4 | 1 | 1.3(3) | 3:2 |
| **NAX035** | 3 | 2 | 3.9(6) | 1:2 |
| **NAX053** | 4 | 2 | 1.1(3) | 3:2 |

1:1). The data in Table 1 highlight that the interactions between Tel24 and the derivatives are slightly better than for BER.

Notably, in the presence of an equal number of phenyl pendant groups, the $K_d$ values decrease as a consequence of the length of the alkyl chain pending from the ligands (3.9 vs. 1.1 for **NAX035** and **NAX053** and 3.2 vs. 1.3 for **NAX039** and **NAX042**).

On the other hand, the different number of phenyl pendants seems not to affect substantially the $K_d$ values of derivatives showing the same length of the alkyl chain (3.2 vs. 3.9 for **NAX039** and **NAX035** and 1.3 vs. 1.1 for **NAX042** and **NAX053**).

As for the binding stoichiometry, different ratios have been found for almost all the ligands, which in turn differ from the binding stoichiometry found for BER.

Noteworthy, all the berberine derivatives, except **NAX039**, are able to bind two G-quadruplex units in solution. Derivatives **NAX042** and **NAX053** are characterized by the same 3:2 ligand:quadruplex molar ratio as previously reported for other ligands like ellipticine and chelerythrine. The latter compounds were supposed to bind to the extremity and to the interface of two or more contiguous G-quadruplexes.[21,22]

The small differences between the binding constants and the stoichiometry ratios found in our experiments with respect to those previously reported in the literature may be ascribed to the different experimental conditions and the DNA sequences used.[1]

### Circular Dichroism Spectroscopy

Circular Dichroism (CD) spectroscopy can supply qualitative information about changes in the G-quadruplex conformation upon ligand binding. In $K^+$ solutions, the Tel24 sequence folds into a mixed hybrid-1 and hybrid-2 structure, with the hybrid-1 conformation being predominant.[24,25] Room-temperature CD spectra of Tel24 (Figure 2) show a positive peak at 290 nm, a shoulder at 268 nm, and a negative peak at 236 nm, in agreement with previous reports in the literature.[21,22,25] The interaction of Tel24 with BER and its semisynthetic derivatives induces changes in the spectral shape, providing different profiles in CD spectra.

In the presence of increasing concentration of BER (Figure 2A), the intensities of the peak at 290 nm and of the shoulder at 268 nm decrease. At the same time the negative band at 236 nm becomes less negative and an induced CD band appears around 360 nm, as observed also for Tel24 upon binding by the natural alkaloids chelerythrine and ellipticine.[21,22] Spectra of the adduct formed with **NAX039** resemble those from the berberine complex, except for a slight increase in the intensity of the positive band at 290 nm (Figure 2B). In the case of **NAX035** (Figure 2D), the recorded spectra showed only a decrease of the peak intensity at 290 nm and a less evident lowering of the shoulder at 268 nm thus indicating a different behavior of the ligand in the interaction with G4 with respect to the other derivatives. **NAX042** (Figure 2C) and **NAX053** (Figure 2E) induce quite similar variations in the Tel24 CD spectra, which are rather different from those determined by BER and the other berberine derivatives and significantly more pronounced. Both compounds induce the appearance of a wide negative band at around 340 nm, an increase in the intensity of the positive band at 290 nm, a net decrease in the shoulder at 268 nm, and the disappearance of the negative band at 236 nm, which is replaced by a positive band with a maximum around 245 nm. The net change in quadruplex conformation upon ligand binding suggests that both **NAX042** and **NAX053** can effectively induce antiparallel G-quadruplex folding.[26]

Thermal melting curves were recorded using the same experimental conditions used for the room-temperature spectra.

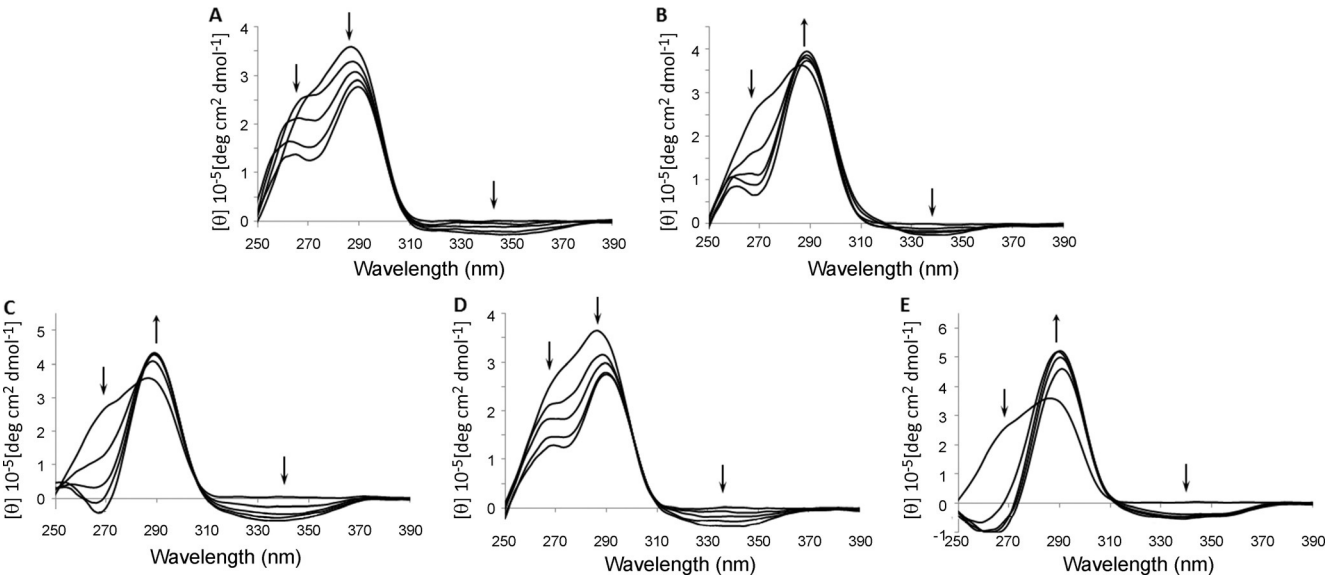


**Figure 2.** CD spectra at 25 °C of Tel24 (56.3 μM) in the presence of 1–4 equivalents of berberine (A), **NAX039** (B), **NAX042** (C), **NAX035** (D), and **NAX053** (E). Solutions prepared in 90 mM LiCl, 10 mM KCl and 10 mM lithium cacodylate (pH 7). The concentration of DMSO was kept constant at 3.75% v/v.

**Table 2.** Analysis of thermal melting curves observed by CD spectroscopy of Tel24 (56.3 μM) in the presence of saturating concentration of berberine and its 13-phenyl and 13-diphenylalkyl derivatives at constant quadruplex:ligand stoichiometric ratio of 1:4. Solutions were prepared in 10 mM lithium cacodylate (pH 7) containing 90 mM LiCl and 10 mM KCl. The concentration of DMSO was kept constant at 3.75% (v/v).

| | $T_m$ [°C] | $\Delta T_m$ [°C] |
|---|---|---|
| DNA alone | 49.9 | 0 |
| BER, Berberine | 61.2 | 11.3 |
| **NAX039** | 61.8 | 11.9 |
| **NAX042** | 61.2 | 11.3 |
| **NAX035** | 56.2 | 6.3 |
| **NAX053** | 61.4 | 11.5 |

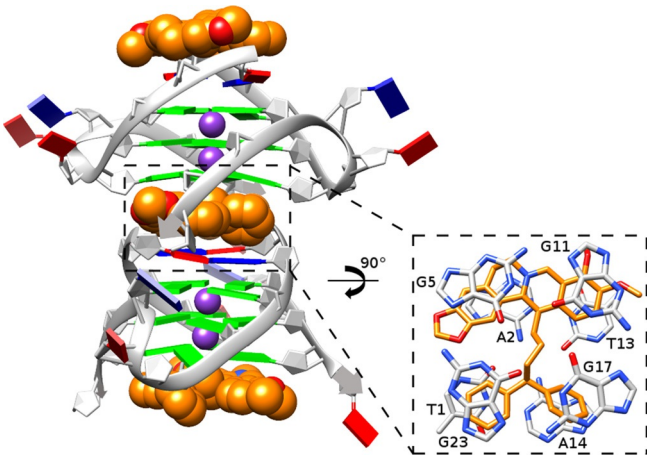


**Figure 3.** Crystal structure of the adduct formed by **NAX053** and the human telomeric sequence Tel12 (1:1 stoichiometric ratio): bimolecular quadruplex units and ligand molecules alternate along parallel columns growing along the [001] direction.

The melting transition was monitored at $\lambda = 290$ nm, and the results are reported in Table 2. Under our experimental conditions, Tel24 shows a single thermal transition at about 49 °C, which is significantly lower than that reported by other authors.[20–22,27] In agreement with previously reported data, we can ascribe the low $T_m$ found for BER to the selected buffer and DMSO concentration used.[20–22,27] Upon ligand binding, the melting temperature of Tel24 increases, thus confirming the ability of the semisynthetic compounds to form stable adducts with the monomolecular telomeric G-quadruplex. An increment of about 11–12 °C characterizes all the ligands studied except **NAX035**, for which a lower $\Delta T_m$ was found ($\Delta T_m = 6.3$ °C).

### X-ray Structure of NAX053-Tel12 Adduct

Crystallization experiments were performed for each semisynthetic derivative of berberine by using two different human telomeric sequences, namely, d[$TAG_3(T_2AG_3)_3$], Tel23, and d[$TAG_3(T_2AG_3)T$], Tel12, which are known to afford monomolecular and bimolecular G-quadruplex structures, respectively.[28] Only for the **NAX053**-Tel12 adduct we obtained satisfactory crystals and were able to solve the structure. As shown in Figure 3, bimolecular quadruplex units and ligand molecules alternate along columns with an overall 1:1 stoichiometric ratio. Each unit consists of parallel-stranded bimolecular quadruplexes featuring three planar stacked G-quartets that are 3.4 Å apart from each other. It is formed by two symmetry-independent Tel12 chains. Potassium ions are found in the internal channel between two adjacent guanine tetrads, located on the crystallographic 4-fold screw axis. Eight guanine carbonyl oxygen atoms are 2.7–3.0 Å apart from each cation, in an overall anti-prismatic coordination environment.

The found parallel folding is in agreement with all the previously reported data obtained by single-crystal X-ray diffraction experiments.[28] On the other hand, it is well known that different kinds of foldings, other than propeller-type, are more easily found in diluted solutions for telomeric DNA, and consequently, the propeller arrangement has been for some time considered to be distinctive of the solid state and to be induced by the crystal packing forces.[29] Nevertheless, this sequence is highly polymorphic in nature, being the obtained folding strongly dependent on the experimental conditions used.[24,30] In particular, some literature reports suggested that, under crowding conditions, telomeric sequences might coexist as an equilibrium mixture of different kinds of arrangements, including also the parallel one;[30,31] in the absence of clear and conclusive evidence about the real form of the telomeric DNA sequence *in vivo*, different arrangements may be taken into account in order to evaluate the possible quadruplex/ligand binding mode.

Among the foldings reported to date, the all parallel one is the only one featuring two external tetrads which are not hindered by adenine and thymine residues.[32] As a matter of fact, in this structure the TTA sequence connecting the guanine tracts in each Tel12 polymer forms a propeller loop which protrudes outwards with respect to the quadruplex core.

The 5′-end thymine and adenine residues from the two chains interact via hydrogen bonds forming an additional tetrad which stacks on the 5′-end G-quartet. The binding site of **NAX053** is defined by the 3′-end G-quartet and the 5′-end TATA platform of two different quadruplex units. The ligand is sandwiched between the two quartets approximately 3.9 Å apart from them (Figures 3 and 4).

**NAX053** interacts via π–π stacking with all the G-tetrad guanines and the TATA platform bases. The berberine core appears quite planar (24° dihedral angle between the A ring, adjacent to the cyclic acetal, and the isoquinoline group of the molecule—C and D rings, Scheme 1), whereas the two phenyl groups of the pendant benzhydryl alkyl moiety are not coplanar, giving rise to a dihedral angle of about 46°, and the alkyl chain is directed toward the G-quartet. Most likely, that induces a steric hindrance which determines the deviation from planarity observed for both the 3′-end G-quartet and the TATA platform at the 5′-end.

In fact, the TATA platform is characterized by dihedral angles in the range 7–14° between each adenine and the adjacent thymine residues, whereas similar angular values can be mea-

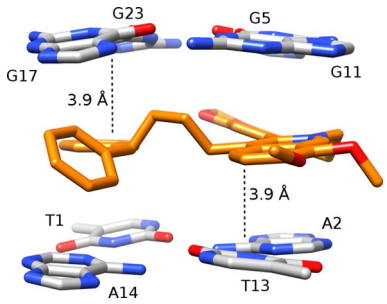


**Figure 4.** The binding site of **NAX053** is defined by the 3′-end G-quartet and the 5′-end TATA platform whose bases interact via π–π stacking with the ligand molecule at an average distance of 3.9 Å.

sured for the guanines at the 5′-end quartet, falling in the range 14–19°.

As a consequence of this loss of planarity, the π–π stacking interactions are optimized despite the evident steric hindrance relative to the alkyl moiety. The crystal structure of the adduct formed by berberine and the human telomeric sequence $d[TAG_3(T_2AG_3)_3]$ (Tel23) is the most significant to be compared with the structure obtained in this work.[11]

This adduct shows the presence of two different binding sites, one defined by two 5′-end G-quartets and the other one by the 3′-end G-quartet and a TA base pair from a symmetry-related quadruplex. Both binding sites are filled by two coplanar berberine molecules stacked on the quartets in such way that they define an approximate four-sided polygon which leaves a free central channel, just above the potassium ions. It is noteworthy that in the **NAX053**-Tel12 adduct, the berberine core is placed on the 3′-end quartet in a strictly similar way with respect to that seen in the adduct of BER with Tel23 (Figure 5). Actually, the alkaloid skeleton of **NAX053** gives rise to π–π stacking interactions with only two guanine residues in the 3′-end quartet, and points its cationic nitrogen toward one of the lateral TTA loops, far from the negative charges on the carbonyl oxygens in the central channel.

## Cytotoxic Activity on Cancer Cells

The effect of NAX derivatives on cell proliferation was evaluated by using the MTT metabolic assay, which measures mitochondrial activity providing a rapid and sensitive way to quantitatively measure cell proliferation and drug cytotoxicity.[33] By applying this test, we have recently demonstrated that the BER derivative **NAX053** has a strong impact on the viability of human colon cancer cells, leading to a well-defined type of cell death.[33] Remarkably, we have observed that the lead compound BER significantly decreases cell viability only at very high concentrations, being less effective than all derivatives on the different cancer cell lines.[33] Here, we extended our analysis to two additional human cancer cell lines, that is, HeLa (derived from uterine cervix carcinoma) and MCF-7 (from breast carcinoma), previously used by other investigators to test effects of BER.[9d,34]

The results illustrated in Figure 6 (upper part) highlight the property of **NAX053** to affect the viability of both cancer cell lines in a dose-dependent manner and more efficiently than the lead compound BER (not shown). In particular, the $IC_{50}$ values of **NAX053** are 2.56 ± 0.098 μM and 2.27 ± 0.015 μM for HeLa and MCF-7 cells, respectively, compared to 18.82 ± 1.267 μM and 11.75 ± 1.138 of BER. These promising data prompted us to analyze also the cytotoxic effect of **NAX042** on a panel of human cancer cell lines, including MCF-7, melanoma A375 and two colon carcinoma cells (SW613-B3 and HCT116). As shown in Figure 6 (lower part), **NAX042** exerts a dose-dependent effect on the viability of all the tested cancer cell lines, which are characterized by telomerase reactivation, having an epithelial origin like HeLa cells. Further experiments could be planned to address the impact of BER derivatives **NAX042** and **NAX053** on cancer mesenchymal cells, such as sarcomas, where mainly the alternative lengthening of telomeres (ALT) mechanism is mainly responsible for telomere elongation.[35] On the whole, our results support the possible use of **NAX042** and **NAX053**, which are even more potent than BER, as anticancer drugs.

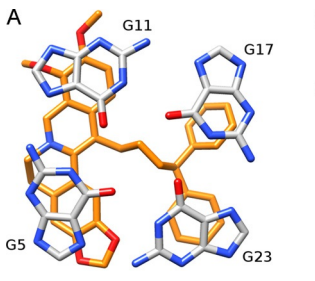


**Figure 5.** The binding site on the 3′-end G-quartet of **NAX053** (A) and of berberine (B) in their respective crystal structures with Tel12 and Tel23.

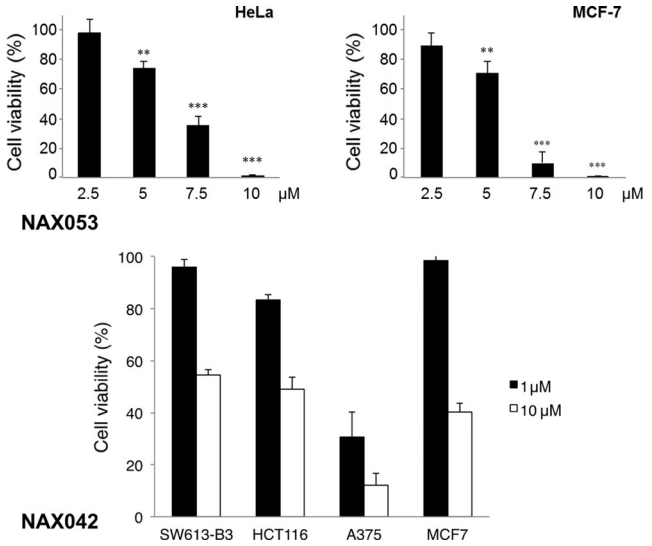


**Figure 6.** Effect of **NAX053** and **NAX042** on cancer cell viability. Four increasing concentrations of **NAX053** (upper panel) and 1 μM/10 μM of **NAX042** (lower panel) were used for 24 h treatments in quadruplicate (three independent MTT experiments were carried out). Data obtained from untreated control cells were considered as 100% to normalize the absorbance of treated samples and are expressed as mean ± SD. $^{**}P < 0.01$; $^{***}P < 0.001$.

## Conclusions

In summary, the interaction between 13-phenylalkyl and 13-diphenylalkyl berberine derivatives and human telomeric sequences folded into G-quadruplexes has been confirmed by both spectroscopic and crystallographic data. All of them somewhat improve the performance of the natural precursor berberine with regard to G-quadruplex binding. **NAX042** and **NAX053** have shown the strongest interactions with human telomeric G-quadruplexes, inducing strong changes in the CD spectral profile.

Stoichiometry ratios derived from spectrophotometric titrations suggest that **NAX042**, **NAX035** and **NAX053** can bind multiple G4 structures in solution as previously reported for other similar alkaloids supposed to bind to the extremity and to the interface of two or more contiguous G-quadruplexes. This hypothesis is supported by the crystal structure of the **NAX053**-Tel12 adduct, despite the apparently different stoichiometry ratio. As a matter of fact, the crystal structure shows the ligand interacting via π-stacking, sandwiched at the interface of two symmetry-related quadruplex units. As a consequence, the binding modes pointed out by our solid-state and solution study results seem to converge toward the hypothesis of a ligand molecule sandwiched between guanine quartets belonging to different quadruplex units. Noteworthy, the berberine core of compound **NAX053** interacts with the 3′-end G-quartet strictly resembling the binding mode of berberine in its adduct with Tel23 in the solid state. The benzhydryl group contributes to the overall stability of the adduct, as it gives additional π-stacking interactions with the DNA residues.

In agreement with these findings, measurements of the cytotoxic activity of the semisynthetic derivatives towards a panel of human cancer cell lines highlighted that **NAX042** and **NAX053** affect the viability of several cancer cell lines characterized by telomerase reactivation, which is a hallmark of most cancer cells, thus suggesting their possible use as anticancer drugs. Remarkably, we found that **NAX042** and **NAX053** are more cytotoxic than the lead compound BER.

## Experimental Section

### Experimental Details

**Synthesis and characterization of the 13-(di)arylalkyl derivatives.** The 13-(di)arylalkyl berberine derivatives are proprietary compounds,[19] and were synthesized starting from commercial berberine chloride and the appropriate (di)arylalkylcarboxaldehydes via a modification of an unusual enamine–aldehyde condensation performed on 7,8-dihydroberberine (Scheme 2).[36]

The aldehydes were prepared starting from commercial (di)arylalkyl alcohols following usual oxidation methods and, when required, homologation procedures known in organic chemistry. The purity (>95%) of the derivatives was assessed by HPLC on a Jasco system LC- 2000 series (Jasco, Europe) with an Agilent Eclipse XDB-C18 (4.6 mm x 150 mm×3.5 mm) column (Agilent Technologies, USA). The flow rate of the mobile phase (50% water, 50% acetonitrile plus 0.1% trifluoroacetic acid) was maintained at 1 mL min$^{-1}$. The absorbance was measured at 235, 265, 340, and 420 nm, and

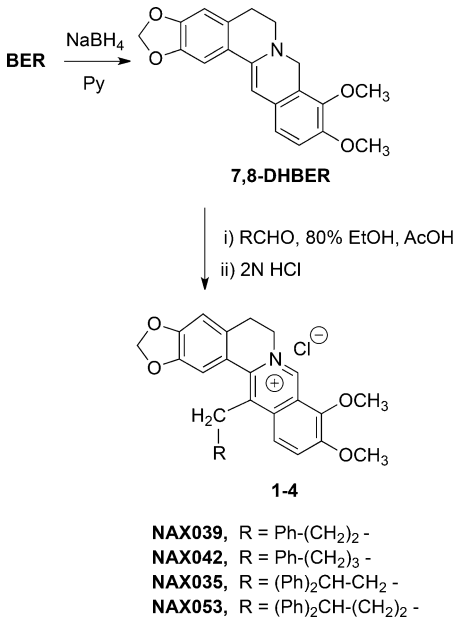


**Scheme 2.** General synthesis of berberine derivatives.

retention times (rt) were measured in minutes. The structures of the derivatives were confirmed by $^1$H NMR spectra recorded on a Varian Mercury 200 MHz spectrometer (Varian, Inc., Palo Alto, USA) from [D$_6$]DMSO solutions or on a Bruker Advance 400 MHz spectrometter (Bruker BioSpin GmbH, Karlsruhe, Germany) from $CDCl_3$ solutions. $^{13}$C NMR spectra were recorded in [D$_6$]DMSO using a Bruker Advance III 400 MHz spectrometer. After 20-fold dilution with $H_2O/CH_3CN$ (1/1) of the 20 mM DMSO solutions, ESI-HRMS spectra were recorded by direct introduction of the samples at a flow rate of 5 μL min$^{-1}$ in an Orbitrap high-resolution mass spectrometer (Thermo, San Jose, CA, USA). The instrument was calibrated just before analyses (external calibration). The working conditions were the following: positive polarity, spray voltage 5 kV, capillary voltage 35 V, capillary temperature 275 °C, tube lens voltage 110 V. The sheath and the auxiliary gases were set, respectively, at 8 (arbitrary units) and 3 (arbitrary units). Xcalibur 2.0. software (Thermo) was used for spectra acquisition and a nominal resolution (at *m/z* 400) of 100 000 was used.

### Materials

The human telomeric sequences d[$(T_2AG_3)_4$] (Tel24), d[$TAG_3(T_2AG_3)_3$] (Tel23) and d[$TAG_3(T_2AG_3)T$] (Tel12) were purchased from Jena Bioscience (Jena, Germany) and used without further purification.

Berberine chloride hydrate (ca. 17% $H_2O$) was purchased from Shanghai Trust&We, Ltd. (Shanghai, China). The mono- and bi- phenylalkyl berberine derivatives were synthetized as described above.

### Preparation of stock solutions

The oligonucleotides were dissolved to a concentration of 1 mM in 50 mM KCl and 20 mM potassium cacodylate buffer (pH 6.5) and then heated to 90 °C for 15 min. The solutions were left to cool overnight to room temperature in order to induce quadruplex formation.

The compounds were dissolved in DMSO to a concentration of 20 mM (stock solution). Milli-Q water from Millipore Water System (Millipore, USA) and analytical grade reagents were used for pre-

paring working solutions which were also filtered through Sartorius Stedim Biotech filters of 0.2 μm.

### UV/Vis spectroscopic titration

Absorbance spectral studies were performed on a Thermo Scientific Evolution 220 UV-vis spectrophotometer (Waltham, MA, USA) at 25 °C. Every experiment was conducted in 150 mM KCl and 10 mM potassium phosphate buffer at pH 7. Matched quartz cells (Hellma, Germany) of 1 cm path length were used. The Tel24 concentration was determined by using $\varepsilon_{260nm} = 244\,600\ M^{-1}cm^{-1}$; for berberine and its semisynthetic derivatives, $\varepsilon_{345nm} = 22\,500\ M^{-1}cm^{-1}$ and $\varepsilon_{341nm} = 21\,500\ M^{-1}cm^{-1}$, respectively, were used. These values were determined under our experimental conditions and are in agreement with previously published data.[16,17,20,22]

Small aliquots of Tel24 solution were added to a solution of ligand at known concentration (~5 μM) until saturation was reached. Equal additions were made to a reference cell during each titration. Readings were noted 5 min after each addition and subsequent mixing in order to guarantee the homogeneous adduct formation. The parameters used for recording spectra are listed as follows: spectral range 400–240 nm, scan speed 100 nm min$^{-1}$, bandwidth 1 nm, integration time 0.6 s, data interval 1 nm. The variation in peak intensity at about 340 nm for the ligands was used to construct the binding isotherm following the method reported by Ghosh and co-workers.[20–22] Briefly, the isotherms were constructed by plotting $\Delta A/\Delta A_{max}$ at the chosen wavelength as a function of increasing quadruplex concentration. The experimental points were fitted by using Equation (1):

$$C_0(\Delta A/\Delta A_{max})^2 - (C_0 + C_p + K_d)(\Delta A/\Delta A_{max}) + C_p = 0 \quad (1)$$

where $C_0$ is the concentration of ligand, $\Delta A$ is the variation in absorbance at the chosen wavelength after each quadruplex addition, $\Delta A_{max}$ is the $\Delta A$ value at ligand saturation, and $C_p$ is the quadruplex concentration. The intercept on the abscissa at $\Delta A/\Delta A_{max} = 0.5$ gives the dissociation constant $K_d$. $\Delta A_{max}$ was obtained from the plot $1/\Delta A$ vs. $1/(C_p\text{-}C_0)$ using Equation (2):

$$1/\Delta A = 1/\Delta A_{max} + 1/(C_p\text{-}C_0) \quad (2)$$

The binding stoichiometry was estimated from the interception of straight lines resulting from fitting of the experimental points belonging to the initial and the saturation regions of the isotherm. The quadruplex concentration at the interception was thus divided by the concentration of the ligand to yield the binding stoichiometry.

### Circular Dichroism Spectroscopy

CD spectra were recorded on a Jasco J-810 Spectropolarimeter (Jasco Cooperation, Tokyo, Japan) equipped with a Peltier temperature controller (model JWJTC-484). Matched quartz cells (Hellma, Germany) of 0.1 cm path length were used. Solutions at known concentration of Tel24 (56.3 μM) were prepared increasing the ligand concentration up to ligand:quadruplex ratio of 4:1. Solutions were prepared in 90 mM LiCl, 10 mM KCl and 10 mM lithium cacodylate at pH 7. For each solution, CD spectra at 25 °C and thermal melting curves were recorded. The technical parameters of the experiments are listed as follows. CD spectra: spectral range 400–230 nm, scan speed 100 nm min$^{-1}$, bandwidth 0.5 nm, data pitch 0.5 nm, time constant 1 s, 6 accumulations. Melting curves: $\lambda =$ 290 nm, temperature slope 90 °C h$^{-1}$, bandwidth 0.5 nm, data pitch 0.2 °C, delay time 0 s, time constant 1 s.

### Crystallization

A search for crystallization conditions was planned based on the work of Campbell and Parkinson using the sitting drop vapor diffusion method.[37] Crystallization experiments were performed for the adducts formed by each semisynthetic derivative of berberine and the human telomeric sequences Tel23 and Tel12, however, only crystals for **NAX053**-Tel12 were obtained by mixing 1 μL of **NAX053** and Tel12 solution in 1:2 stoichiometric ratio at concentration of 1 mM with 1 μL of 1 M $(NH_4)_2SO_4$, 0.05 M $Li_2SO_4$ and 0.05 M sodium cacodylate at pH 6.5 and equilibration against 100 μL of 2.4 M $(NH_4)_2SO_4$ solution at $T = 23$ °C. Yellow prismatic crystals were observed after two weeks upon drops deposition.

### Data collection and structure refinement

Diffraction experiments on the crystals were performed at 100 K, using as cryoprotectant the crystallization condition supplemented with 30% v/v glycerol. Data were collected at the ID23-1 beam-line (ESRF, Grenoble) up to a maximum resolution of 1.70 Å, using 1.000 Å wavelength X-ray. Data were integrated and scaled using the program XDS.[38] The structure of the adduct was solved by molecular replacement using the program Phaser.[39] The crystallographic coordinates of the Tel12-coptisine adduct were used, as a search model, after deleting atoms belonging to ligand and solvent molecules (PDB accession number 4P1D). The $F_O$-$F_C$ electron density maps showed a clear density for the drug molecule located on a 4-fold screw axis. The T18 and T24 thymine residues are disordered and they have been only partially localized in the crystal structure. The model was refined using the program Refmac5 from the CCP4 package.[40] Thermal factors were treated as isotropic. The **NAX053** molecule was built by using the program JLigand and added manually into the electronic density maps.[41] Manual rebuilding of the model was performed using the program Coot.[42] The crystal packing analysis was made by means of the Mercury program.[43] Final coordinates and structure factors have been deposited with the Protein Data Bank (PDB accession number 5CDB). Statistics of the data collection and refinement are reported in Table S1 in the Supporting Information.

### Evaluation of cytotoxic activity on cancer cells

Human HeLa (uterine cervix carcinoma), A375 (melanoma), SW613-B3 and HCT116 (colon carcinoma), and MCF-7 (breast carcinoma) cell lines were grown at 37 °C and 5% $CO_2$ atmosphere, in Dulbecco's modified Eagle's medium (DMEM) supplemented with 10% FBS, 0.1 mg mL$^{-1}$ penicillin, 100 U mL$^{-1}$ streptomycin, 2 mM glutamine and 2% sodium pyruvate (all reagents were from Celbio, Milano, Italy). Twenty-four hours after seeding, cells were treated for 24 h with the BER derivative **NAX042** or **NAX053** (stock solutions: 10 mM in DMSO) at different concentrations. Cell viability was analyzed by the MTT metabolic assay, which measures mitochondrial activity, by applying a previously reported procedure.[33] Briefly, $2\times10^3$ cells were seeded in 96-multiwell plates and, 24 h later, incubated for 24 h with increasing concentrations (1–10 μM) of **NAX053**. At the end of the incubation, 20 μL of Cell Titer 96 AQueous One Solution Cell Proliferation Reagent (Promega Italia, Milano, Italy) were added to each well. The plates were then maintained for 4 h at 37 °C; the absorbance of each sample was measured with a microplate reader (EZ Red 400, Biochrom, Cambridge, UK) at 492 nm. Experiments were performed in quadruplicate and

repeated three times. The ANOVA and Dunnett's multiple comparison tests have been applied. Statistical analysis was performed using GraphPad Prism 5.0.

## Acknowledgements

Ente Cassa di Risparmio di Firenze, Italy, is gratefully acknowledged for a grant to F.P. (2014.0309). Naxospharma srl, Italy, acknowledges financial support by the Italian Ministry of Economic Development, Grant no. 01705, awarded within the sixth call of the EuroTransBio initiative, Project BER.T.A. Luis Miguel Guamán Ortiz was a Ph.D. student (Dottorato in Genetica, Biologia Cellulare e Molecolare, University of Pavia, Italy) supported by SENESCYT (Quito, Ecuador) and Universidad Tecnica Particular de Loja (Loja, Ecuador).

**Keywords:** alkaloids · berberine · crystal structure · G-quadruplexes · telomeric DNA · X-ray diffraction

[1] a) J. Qiu, M. Wang, Y. Zhang, P. Zeng, T. M. Ou, J. H. Tan, S. L. Huang, L. K. An, H. Wang, L. Q. Gu, Z. S. Huang, D. Li, *Curr. Top. Med. Chem.* **2015**, *15*, 1971 – 1987; b) S. Balasubramanian, *Bioorg. Med. Chem.* **2014**, *22*, 4356 – 4370; c) J. P. Taylor, *Nature* **2014**, *507*, 175 – 177; d) J. Bidzinska, G. Cimino-Reale, N. Zaffaroni, M. Folini, *Molecules* **2013**, *18*, 12368 – 12395; e) T. Shalaby, G. Fiaschetti, K. Nagasawa, K. Shin-ya, M. Baumgartner, M. Grotzer, *Molecules* **2013**, *18*, 12500 – 12537; f) S. Burge, G. N. Parkinson, P. Hazel, A. K. Todd, S. Neidle, *Nucleic Acids Res.* **2006**, *34*, 5402 – 5415.

[2] P. Murat, S. Balasubramanian, *Curr. Opin. Genetics Dev.* **2014**, *25*, 22 – 29.

[3] M. Kaushik, S. Kaushik, A. Bansal, S. Saxena, S. Kukreti, *Curr. Mol. Med.* **2011**, *11*, 744 – 769.

[4] a) E. Y. N. Lam, D. Beraldi, D. Tannahill, S. Balasubramanian, *Nat. Commun.* **2013**, *4*, 1796 – 1803; b) G. Biffi, D. Tannahill, J. McCafferty, S. Balasubramanian, *Nature Chem.* **2013**, *5*, 182 – 186; c) G. Biffi, M. Di Antonio, D. Tannahill, S. Balasubramanian, *Nature Chem.* **2014**, *6*, 75 – 80; d) L. Yuan, T. Tian, Y. Chen, S. Yan, X. Xing, Z. Zhang, Q. Zhai, L. Xu, S. Wang, X. Weng, B. Yuan, Y. Feng, X. Zhou, *Sci. Rep.* **2013**, *3*, 1811; e) R. F. Hoffmann, Y. M. Moshkin, S. Mouton, N. A. Grzeschik, R. D. Kalicharan, J. Kuipers, A. H. G. Wolters, K. Nishida, A. V. Romashchenko, J. Postberg, H. Lipps, E. Berezikov, O. C. M. Sibon, B. N. G. Giepmans, P. M. Lansdorp, *Nucleic Acids Res.* **2015**, *44*, 152 – 165.

[5] a) S. Balasubramanian, S. Neidle, *Curr. Opin. Chem. Biol.* **2009**, *13*, 345 – 353; b) S. N. Georgiades, N. H. A. Karim, K. Suntharalingam, R. Vilar, *Angew. Chem. Int. Ed.* **2010**, *49*, 4020 – 4034; c) B. Maji, S. Bhattacharya, *Chem. Commun.* **2014**, *50*, 6422 – 6438; d) S. A. Ohnmacht, S. Neidle, *Bioorg. Med. Chem. Lett.* **2014**, *24*, 2602 – 2612; e) J. Zhang, F. Zhang, H. Li, C. Liu, J. Xia, L. Ma, W. Chu, Z. Zhang, C. Chen, S. Li, S. Wang, *Curr. Med. Chem.* **2012**, *19*, 2957 – 2975.

[6] a) Y. Lu, W. Leong, O. Guérin, E. Gilson, J. Ye, *Front. Med.* **2013**, *7*, 411 – 417; b) M. Ruden, N. Puri, *Cancer Treat. Rev.* **2013**, *39*, 444 – 456.

[7] M. Tillhon, L. M. Guamán Ortiz, P. Lombardi, A. I. Scovassi, *Biochem. Pharmacol.* **2012**, *84*, 1260 – 1267.

[8] a) M. Chu, R. Xiao, Y. Yin, X. Wang, Z. Chu, M. Zhang, R. Ding, Y. Wang, *Clin. Microbiol. Open Access* **2014**, *3*, 1000150; b) Y. Hu, E. A. Ehli, J. Kittelsrud, P. J. Ronan, K. Munger, T. Downey, K. Bohlen, L. Callahan, V. Munson, M. Jahnke, L. L. Marshall, K. Nelson, P. Huizenga, R. Hansen, T. J. Soundy, G. E. Davies, *Phytomedicine* **2012**, *19*, 861 – 867; c) H. F. Ji, L. Shen, *Molecules* **2011**, *16*, 6732 – 6740; d) M. Kim, K. H. Cho, M. S. Shin, J. M. Lee, H. S. Cho, C. J. Kim, D. H. Shin, H. J. Yang, *Int. J. Mol. Med.* **2014**, *33*, 870 – 878; e) S. K. Kulkarni, A. Dhir, *Phytother. Res.* **2010**, *24*, 317 – 324; f) X. H. Zeng, X. J. Zeng, Y. Y. Li, *Am. J. Cardiol.* **2003**, *92*, 173 – 176; g) W. Zha, G. Liang, J. Xiao, E. J. Studer, P. B. Hylemon, W. M. Pandak, Jr., G. Wang, X. Li, H. Zhou, *PLoS ONE* **2010**, *5*, e9069; h) M. Zhang, L. Chen, *Acta Pharm. Sin. B* **2012**, *2*, 379 – 386; i) X. Q. Zhou, X. N. Zeng, H. Kong, X. L. Sun, *Neurosci. Lett.* **2008**, *447*, 31 – 36.

[9] a) Y. Sun, K. Xun, Y. Wang, X. Chen, *Anticancer Drugs* **2009**, *20*, 757 – 769; b) S. K. Mantena, S. D. Sharma, S. K. Katiyar, *Mol. Cancer Ther.* **2006**, *5*, 296 – 308; c) Z. Liu, Q. Liu, B. Xu, J. Wu, C. Guo, F. Zhu, Q. Yang, G. Gao, Y. Gong, C. Shao, *Mutat. Res. Fund. Mol. Mech. Mut.* **2009**, *662*, 75 – 83; d) J. B. Patil, J. Kim, G. K. Jayaprakasha, *Eur. J. Pharmacol.* **2010**, *645*, 70 – 78; e) S. Mahata, A. C. Bharti, S. Shukla, A. Tyagi, S. A. Husain, B. C. Das, *Mol. Cancer* **2011**, 10:39; f) X. Hu, X. Wu, Y. Huang, Q. Tong, S. Takeda, Y. Qing, *Mol. Med. Rep.* **2014**, *9*, 1883 – 1888; g) H. L. Wu, C. Y. Hsu, W. H. Liu, B. Y. M. Yung, *Int. J. Cancer* **1999**, *81*, 923 – 929; h) Y. Wang, M. M. Kheir, Y. Chai, J. Hu, D. Xing, F. Lei, L. Du, *PLoS ONE* **2011**, *6*, e23495; i) J. Li, L. Gu, H. Zhang, T. Liu, D. Tian, M. Zhou, S. Zhou, *Lab. Invest.* **2013**, *93*, 354 – 364; j) L. M. Guamán Ortiz, P. Lombardi, M. Tillhon, A. I. Scovassi, *Molecules* **2014**, *19*, 12349 – 12367; k) K. H. Lee, H. L. Lo, W. C. Tang, H. H. Hsiao, P. M. Yang, *Sci. Rep.* **2014**, *4*, 6394 – 6402.

[10] a) N. K. Sharma, P. Lunawat, M. Dixit, *Am. J. Biochem. Biotechnol.* **2011**, *7*, 130 – 134; b) K. Bhadra, G. S. Kumar, *Biochim. Biophys. Acta* **2011**, *1810*, 485 – 496; c) A. Arora, C. Balasubramanian, N. Kumar, S. Agrawal, R. P. Ojha, S. Maiti, *FEBS J.* **2008**, *275*, 3971 – 3983.

[11] C. Bazzicalupi, M. Ferraroni, A. R. Bilia, F. Scheggi, P. Gratteri, *Nucleic Acids Res.* **2013**, *41*, 632 – 638.

[12] I. Bessi, C. Bazzicalupi, C. Richter, H. R. A. Jonker, K. Saxena, C. Sissi, M. Chioccioli, S. Bianco, A. R. Bilia, H. Schwalbe, P. Gratteri, *ACS Chem. Biol.* **2012**, *7*, 1109 – 1119.

[13] D. Bhowmik, G. S. Kumar, *Mini Rev. Med. Chem.* **2015**, *16*, 104 – 119.

[14] a) W. J. Zhang, T. M. Ou, Y. J. Lu, Y. Y. Huang, W. B. Wu, Z. S. Huang, J. L. Zhou, K. Y. Wong, L. Q. Gu, *Bioorg. Med. Chem.* **2007**, *15*, 5493 – 5501; b) Y. Ma, T. M. Ou, J. Q. Hou, Y. J. Lu, J. H. Tan, L. Q. Gu, Z. S. Huang, *Bioorg. Med. Chem.* **2008**, *16*, 7582 – 7591; c) Y. Ma, T. M. Ou, J. H. Tan, J. Q. Hou, S. L. Huang, L. Q. Gu, Z. S. Huang, *Bioorg. Med. Chem. Lett.* **2009**, *19*, 3414 – 3417; d) K. C. Gornall, S. Samosorn, B. Tanwirat, A. Suksamrarn, J. B. Bremner, M. J. Kelso, J. L. Beck, *Chem. Commun.* **2010**, *46*, 6602 – 6604; e) Y. Ma, T. M. Ou, J. H. Tan, J. Q. Hou, S. L. Huang, L. Q. Gu, Z. S. Huang, *Eur. J. Med. Chem.* **2011**, *46*, 1906 – 1913; f) M. Tera, T. Hirokawa, S. Okabe, K. Sugahara, H. Seimiya, K. Shimamoto, *Chem. Eur. J.* **2015**, *21*, 14519 – 14528; g) K. Iwasa, M. Moriyasu, T. Yamori, T. Turuo, D. U. Lee, W. Wiegrebe, *J. Nat. Prod.* **2001**, *64*, 896 – 898.

[15] M. L. Waters, *Curr. Opin. Chem. Biol.* **2002**, *6*, 736 – 741.

[16] D. Bhowmik, M. Hossain, F. Buzzetti, R. D'Auria, P. Lombardi, G. S. Kumar, *J. Phys. Chem. B* **2012**, *116*, 2314 – 2324.

[17] a) D. Bhowmik, F. Buzzetti, G. Fiorillo, L. Franchini, T. M. Syeda, P. Lombardi, G. S. Kumar, *J. Therm. Anal. Calorim.* **2014**, *118*, 461 – 473; b) D. Bhowmik, F. Buzzetti, G. Fiorillo, P. Lombardi, G. S. Kumar, *Spectrochim. Acta A* **2014**, *120*, 257 – 264.

[18] D. Bhowmik, F. Buzzetti, G. Fiorillo, F. Orzi, T. M. Syeda, P. Lombardi, G. S. Kumar, *Med. Chem. Commun.* **2014**, *5*, 226 – 231.

[19] US Patent No. 1, 881, 09B2 to Naxospharma S. R. L., Italy, **2012**.

[20] S. Ghosh, S. K. Pradhan, A. Kar, S. Chowdhury, D. Dasgupta, *Biochim. Biophys. Acta* **2013**, *1830*, 4189 – 4201.

[21] S. Ghosh, J. Jana, R. K. Kar, S. Chatterjee, D. Dasgupta, *Biochemistry* **2015**, *54*, 974 – 986.

[22] S. Ghosh, A. Kar, S. Chowdhury, D. Dasgupta, *Biochemistry* **2013**, *52*, 4127 – 4137.

[23] D. Bhowmik, G. Fiorillo, P. Lombardi, G. S. Kumar, *J. Mol. Recognit.* **2015**, *28*, 722 – 730.

[24] a) J. Dai, M. Carver, D. Yang, *Biochimie* **2008**, *90*, 1172 – 1183; b) K. N. Luu, A. T. Phan, V. Kuryavyi, L. Lacroix, D. J. Patel, *J. Am. Chem. Soc.* **2006**, *128*, 9963 – 9970; c) A. T. Phan, K. N. Luu, D. J. Patel, *Nucleic Acids Res.* **2006**, *34*, 5715 – 5719; d) A. T. Phan, V. Kuryavyi, K. N. Luu, D. J. Patel, *Nucleic Acids Res.* **2007**, *35*, 6517 – 6525.

[25] S. K. Pradhan, D. Dasgupta, G. Basu, *Biochem. Biophys. Res. Commun.* **2011**, *404*, 139 – 142.

[26] a) M. Vorlíčková, I. Kejnovská, J. Sagi, D. Renčiuk, K. Bednářová, J. Motlová, J. Kypr, *Methods* **2012**, *57*, 64 – 75; b) A. Randazzo, G. P. Spada, M. W. da Silva, *Top. Curr. Chem.* **2013**, *330*, 67 – 86.

[27] C. Antonacci, J. B. Chaires, R. D. Sheardy, *Biochemistry* **2007**, *46*, 4654 – 4660.

[28] G. W. Collie, N. H. Campbell, S. Neidle, *Nucleic Acids Res.* **2015**, *43*, 4785 – 4799.

[29] J. Li, J. J. Correia, L. Wang, J. O. Trent, J. B. Chaires, *Nucleic Acids Res.* **2005**, *33*, 4649 – 4659.

[30] a) A. N. Lane, J. B. Chaires, R. D. Gray, J. O. Trent, *Nucleic Acids Res.* **2008**, *36*, 5482 – 5515; b) K. Zheng, Z. Chen, Y. Hao, Z. Tan, *Nucleic Acids Res.* **2010**, *38*, 327 – 338; c) L. Xu, S. Feng, X. Zhou, *Chem. Commun.* **2011**, *47*, 3517 – 3519; d) L. Petraccone, A. Malafronte, J. Amato, C. Giancola, *J. Phys. Chem. B* **2012**, *116*, 2294 – 2305; e) L. Petraccone, B. Pagano, C. Giancola, *Methods* **2012**, *57*, 76 – 83; f) H. T. Le, W. L. Dean, R. Buscaglia, J. B. Chaires, J. O. Trent, *J. Phys. Chem. B* **2014**, *118*, 5390 – 5405; g) L. Petraccone, C. Spink, J. O. Trent, N. C. Garbett, C. S. Mekmaysy, C. Giancola, J. B. Chaires, *J. Am. Chem. Soc.* **2011**, *133*, 20951 – 20961; h) H. Yu, X. Gu, S. Nakano, D. Miyoshi, N. Sugimoto, *J. Am. Chem. Soc.* **2012**, *134*, 20060 – 20069.

[31] a) D. Renčiuk, I. Kejnovská, P. Školáková, K. Bednářová, J. Motlová, M. Vorlícková, *Nucleic Acids Res.* **2009**, *37*, 6625 – 6634; b) L. Martino, B. Pagano, I. Fotticchia, S. Neidle, C. Giancola, *J. Phys. Chem. B* **2009**, *113*, 14779 – 14786; c) R. Hänsel, F. Löhr, S. Foldynová-Trantírková, E. Bamberg, L. Trantírek, V. Dötsch, *Nucleic Acids Res.* **2011**, *39*, 5768 – 5775; d) B. Heddi, A. T. Phan, *J. Am. Chem. Soc.* **2011**, *133*, 9824 – 9833; e) R. Hänsel, F. Löhr, L. Trantírek, V. Dötsch, *J. Am. Chem. Soc.* **2013**, *135*, 2816 – 2824.

[32] S. M. Haider, I. Autiero, S. Neidle, *Biochimie* **2011**, *93*, 1275 – 1279.

[33] a) L. M. Guamán Ortiz, M. Tillhon, M. Parks, I. Dutto, E. Prosperi, M. Savio, A. G. Arcamone, F. Buzzetti, P. Lombardi, A. I. Scovassi, *Biomed. Res. Int.* **2014**, *2014*, 924585; b) L. M. Guamán Ortiz, A. L. Croce, F. Aredia, S. Sapienza, G. Fiorillo, T. M. Syeda, F. Buzzetti, P. Lombardi, A. I. Scovassi, *Acta Biochim. Biophys. Sin.* **2015**, *47*, 824 – 833.

[34] B. Lu, M. Hu, K. Liu, J. Peng, *Toxicol. in Vitro* **2010**, *24*, 1482 – 1490.

[35] R. L. Dilley, R. A. Greenberg, *Trends Cancer* **2015**, *1*, 145 – 156.

[36] K. Iwasa, M. Kamigauchi, M. Sugiura, H. Nanba, *Planta Med.* **1997**, *63*, 196 – 198.

[37] N. H. Campbell, G. N. Parkinson, *Methods* **2007**, *43*, 252 – 263.

[38] W. Kabsch, *Acta Crystallogr. D* **2010**, *66*, 125 – 132.

[39] A. J. McCoy, R. W. Grosse-Kunstleve, P. D. Adams, M. D. Winn, L. C. Storoni, R. J. Read, *J. Appl. Cryst.* **2007**, *40*, 658 – 674.

[40] a) G. N. Murshudov, A. A. Vagin, E. J. Dodson, *Acta Crystallogr. D* **1997**, *53*, 240 – 255; b) M. D. Winn, C. C. Ballard, K. D. Cowtan, E. J. Dodson, P. Emsley, P. R. Evans, R. M. Keegan, E. B. Krissinel, A. G. W. Leslie, A. McCoy, S. J. McNicholas, G. N. Murshudov, N. S. Pannu, E. A. Potterton, H. R. Powell, R. J. Read, A. A. Vagin, K. S. Wilson, *Acta Crystallogr. D* **2011**, *67*, 235 – 242.

[41] A. A. Lebedev, P. Young, M. N. Isupov, O. V. Moroz, A. A. Vagin, G. N. Murshudov, *Acta Crystallogr. D* **2012**, *68*, 431 – 440.

[42] P. Emsley, B. Lohkamp, W. G. Scott, K. Cowtan, *Acta Crystallogr. D* **2010**, *66*, 486 – 501.

[43] C. F. Macrae, P. R. Edgington, P. McCabe, E. Pidcock, G. P. Shields, R. Taylor, M. Towler, J. van de Streek, *J. Appl. Cryst.* **2006**, *39*, 453 – 457.

Manuscript received: January 28, 2016
Accepted Article published: February 11, 2016
Final Article published: March 11, 2016